Colloids and Surfaces B: Biointerfaces 136 (2015) 74–83

Contents lists available at ScienceDirect

Colloids and Surfaces B: Biointerfaces

journal homepage: www.elsevier.com/locate/colsurfb

Surface modification of zirconia with polydopamine to enhance fibroblast response and decrease bacterial activity *in vitro*: A potential technique for soft tissue engineering applications

Mingyue Liu[a], Jianfeng Zhou[b], Yang Yang[b], Miao Zheng[b], Jianjun Yang[c], Jianguo Tan[b,*]

[a] Outpatient Department, School and Hospital of Stomatology, Peking University, Beijing 100034, China
[b] Department of Prosthodontics, School and Hospital of Stomatology, Peking University, Beijing 100081, China
[c] Department of Oral and Maxillofacial Surgery, The Affiliated Hospital of Medical College, Qingdao University, Qingdao, Shandong, 266001, China

ARTICLE INFO

Article history:
Received 28 October 2014
Received in revised form 22 April 2015
Accepted 24 June 2015
Available online 30 June 2015

Key words:
Zirconia
Surface modification
Polydopamine coating
Implant interface
Cellular response
Bacterial adhesion

ABSTRACT

The quality of soft-tissue integration plays an important role in the short- and long-term success of dental implants. The aim of the present study was to provide a surface modification approach for zirconia implant abutment materials and to evaluate its influence on fibroblast behavior and oral bacteria adhesion, which are the two main factors influencing the quality of peri-implant soft-tissue seal. In this study, polydopamine (PDA)-coated zirconia was prepared and the surface characteristics were evaluated using scanning electron microscopy, atomic force microscopy, a contact-angle-measuring device, X-ray photoelectron spectroscopy, and Raman spectroscopy. The responses of human gingival fibroblasts (HGFs) to PDA-coated zirconia; i.e., adhesion, proliferation, morphology, protein synthesis, and gene expression, were analyzed. Additionally, the adhesion of *Streptococcus gordonii* and *Streptococcus mutans* to zirconia after PDA coating was assessed by scanning electron microscopy and live/dead staining. The material surface analyses suggested the successful coating of PDA onto the zirconia surface. The PDA coating significantly increased cell adhesion and proliferation compared with pristine zirconia. HGFs exhibited a high degree of spreading and secreted a high level of collagen type I on PDA-modified disks. Upregulation of integrin α_5, β_1, β_3 and fibronectin was noted in HGFs cultured on PDA-coated zirconia. The number of adherent bacteria decreased significantly on zirconia after PDA coating. In summary, our result suggest that PDA is able to modify the surface of zirconia, influence HGFs' behavior and reduce bacterial adhesion. Therefore, this surface modification approach holds great potential for improving soft-tissue integration around zirconia abutments in clinical application.

1. Introduction

The use of dental implants as an alternative to certain traditional rehabilitation methods for completely and partially edentulous patients has been widely applied and has achieved a remarkable success. The long-term success of dental implants in terms of form and function depends not only on the integration of the implant into the surrounding bone but also on the quality of soft tissue seal. Previously, most of the advances in dental implant research are about the optimization of osseointegration, but the research on the improvement of peri-implant soft-tissue reactions is relatively less. The soft-tissue seal structure, consisting of epithelium and connective tissue, has been histologically evaluated *in vivo* and is defined as the 'biological width' [1]. It protects the underlying bone and implant from bacterial penetration, prevents the loss of crestal bone, and maintains the normal shape of the gingiva [2]. In extensive investigations of soft tissue responses to oral implant surfaces, it has been shown that physical chemical properties of implant materials significantly influence the quality of soft tissue seal [3]. Therefore, the modification of implant abutment surfaces to promote early formation of enduring and effective soft-tissue barriers has been a focus of investigation.

The main cell type in peri-implant soft tissues is human gingival fibroblasts (HGFs) [4]. Fibroblasts synthesize and maintain the components of the extracellular matrix, are involved in the maintenance of connective tissue homeostasis, and are responsible for tissue repair and regeneration in the wound-healing process [5]. HGFs play an important role in establishing and maintaining the

* Corresponding author at: Department of Prosthodontics, School and Hospital of Stomatology, Peking University, 22# Zhongguancun South Street, Haidian District, Beijing 100081, China. Fax: +86 1082 195531.
E-mail address: tanwume@vip.sina.com (J. Tan).

http://dx.doi.org/10.1016/j.colsurfb.2015.06.047
0927-7765/

mucosal seal of implants [6]. Investigations have suggested that surface modification of implants significantly influences the behavior of fibroblasts – such as adhesion, proliferation, morphology, and differentiation – thereby influencing the reaction of the soft tissue on the implant surface [7–9].

Microbial infection is another main factor influencing peri-implant soft-tissue seal. During and immediately after surgery, bacterial colonization and subsequent biofilm formation occurs on implant surfaces [10]. Such infections are not easy to treat because bacteria are protected by the biofilms, leading to the destruction of adjacent tissue or even implant failure [11]. *Streptococcus* spp. are the predominant initial-colonizing bacteria; colonization by these microorganisms provides a surface suitable for later bacterial colonization [10]. The surface properties of the implant materials – such as roughness, surface free energy, and chemical characteristics – have a marked impact on bacterial accumulation [12]. Therefore, numerous clinical and *in vitro* studies have focused on reducing biofilm formation by modifying implant surfaces. Various surface treatment methods – such as dry ion implantation of F+ [13], deposition of silver ion and titanium (zirconium) nitride [14,15], coating of antibacterial polymers (e.g., silica, chitosan-lauric acid) [16,17] and peptides (e.g., silk, and a multilayered film containing an antimicrobial peptide) [18,19], and immobilization of antibiotics [20] – have been developed to improve the antibacterial properties of implant materials.

Currently, titanium is the most widely used material and has become the gold standard for both implant and abutment due to its excellent mechanical properties and biocompatibility. However, as an abutment, its dark grayish color limits its application in aesthetic zone [21]. Zirconia, introduced as an alternative to titanium, provides a better aesthetic outcome. In addition, it has demonstrated lower bacterial colonization and similar soft-tissue attachment to titanium, possibly providing favorable soft-tissue integration [22,23]. However, the surface of zirconia is bio-inert and difficult to modify. Numerous surface treatment methods to improve the bioactivity of titanium are available; however, such research for zirconia remains in its infancy. Several physical and chemical surface modification techniques have been developed to enhance the bioactivity of zirconia in terms of tissue reactions, such as optimizing the surface texture (sandblasting, acid-etching) [24], ultraviolet irradiation [25], laser application (e.g., Er:YAG, CO_2 or diode laser) [26,27], and coating with micro-arc oxidized zirconia films [28], calcium phosphate [29], or fluor-hydroxyapatite [30]. Among those approaches, the physical methods require specialized equipment and conditions, while bioactive coatings frequently demonstrate poor adhesion to the material and require complex procedures. In addition, most of the above surface modification methods are used to promote osseointegration; few studies have focused on soft-tissue integration. Therefore, there is an urgent need for a simple and effective surface modification method to enhance the bioactivity of zirconia in terms of soft-tissue integration.

3,4-dihydroxy-L-phenylalanine (L-DOPA) was found to be an important component in the adhesive structure of mussels [31]. Dopamine, precursor of L-DOPA, can self-polymerize and adhere strongly to a wide range of organic and inorganic materials. Coating can be achieved by simply dipping objects in an alkaline dopamine solution (e.g., pH 8.5) [32]. Furthermore, polydopamine (PDA) film, which is enriched in catechol and amino groups, provides a surface for secondary reactions via Michael addition or Schiff base chemistry to create multifunctional coatings. Although the molecular mechanism of the polymerization process has not been well documented, the PDA coating technique has been applied in various fields such as energy science, water treatment, sensing, and biomedical science [31]. Because coating does not require a complex procedure, and is solvent-free and non-toxic, it is particularly suitable for biomaterial application. PDA coatings on bio-inert surfaces facilitate protein adsorption and cell adhesion [33–35]. Moreover, PDA has also been employed to fabricate antimicrobial surfaces. Iqbal et al. [36] found that PDA itself has an antimicrobial effect on *Escherichia coli*. Recently, Liu et al. [37] first applied dopamine derivatives (L-DOPA) onto the zirconia surface to promote the osteogenesis of implants. Nevertheless, the influence of PDA coating on the soft-tissue integration of zirconia implants and oral bacterial colonization remains unexplored. In addition, dopamine performs better than L-DOPA in terms of increasing surface hydrophilicity, the index of which is critical for the regulation of cellular and bacterial behavior [38]. Therefore, dopamine coating holds greater potential in terms of improving tissue reactions around zirconia compared with L-DOPA.

The objective of the present study was to enhance the bioactivity of zirconia abutment materials using PDA modification technique. The effects of PDA coating on the behavior of HGFs and bacterial adhesion were investigated *in vitro*. In addition, specific cell adhesion- and differentiation-related genes expressions were detected at molecular level. We hypothesized that PDA can deposit onto zirconia surface and the coating would facilitate the adhesion, proliferation, and differentiation of HGFs and reduce bacterial adhesion.

2. Material and methods

2.1. Specimen preparation

Zirconia disks (Zenostar, Wieland Dental, Germany; 20-mm diameter, 2-mm-thick) were first obtained using a cutting machine. The crystallographic structure of zirconia was analyzed previously and the results suggested that it fitted the properties of zirconium yttrium oxide [25]. Zirconia disks were wet-grinded and polished to an 800-grit SiC abrasive paper. The specimens were successively ultrasonically cleaned using absolute ethanol and distilled water each for 20 min and then dried in the oven at 50 °C before surface treatment.

After polishing, PDA coating was performed as described previously [32]. In brief, the disks were immersed in a dopamine solution (2 mg/mL in 10 mM Tris-HCl, pH 8.5) and gently shaken for 24 h at room temperature. The PDA-coated disks were then rinsed extensively with distilled water to remove unattached dopamine molecules and then dried under a N_2 stream. Zirconia disks were immediately used after coating and denoted as PDA-zirconia. Untreated disks were used as controls. After surface preparation, all disks were sterilized with 75% ethanol for 40 min, washed three times in phosphate-buffered saline (PBS), and then placed into 24-well culture plates for cell and bacterial assays.

2.2. Surface characterization

2.2.1. Surface topography and surface roughness

Atomic force microscopy (AFM) (P9 XPM; NT-MDT, Russia) was used to examine the surface topography of the samples. Peak-to-valley surface roughness (Ra) measurements were taken from the roughness profile. The surface morphologies of the zirconia disks were also observed by scanning electron microscopy (SEM) (S-4800; Hitachi, Tokyo, Japan). Three samples from each group were visualized at five randomly chosen locations per sample.

2.2.2. Surface wettability

The surface wettability of the substrates was determined by the contact angle of a 1 μl double-distilled water droplet measured using a contact-angle-measuring device (SL200; USA Kino Indus-

try). Five measurements from different regions of each sample were taken and each group contained three samples.

2.2.3. Chemical composition

The chemical composition of the coating was analyzed using X-ray photoelectron spectroscopy (XPS) (ESCALAB 250; ThermoFisher Scientific, Waltham, USA) and Raman spectroscopy (RM 2000; Renishaw, UK). For the XPS examination, the binding energies for all of the spectra were calibrated using the C 1s peak (284.6 eV), and the survey spectra were collected within the range 0–600 eV.

2.3. Cellular response

2.3.1. Cell culture

Primary HGFs were grown from tissue explants. Briefly, gingival tissue obtained from patients who underwent periodontal surgery was cut into minced pieces (~1 mm^3) and placed in 35-mm cell culture dishes containing Dulbecco's modified Eagle's medium (DMEM; Gibco, Gaithersburg, USA) supplemented with 10% fetal bovine serum (FBS; Gibco) and 2% antibiotic-antimycotic solution (Gibco). Fibroblasts were obtained by trypsinization of the primary outgrowth of cells, and were maintained and routinely passaged in 10-cm dishes in DMEM with 10% FBS and 1% antibiotic–antimycotic solution at 37 °C under a humidified atmosphere of 5% CO_2 in 95% air. Cells at the third to sixth passage were used for the experiments as follows. Informed consent was provided by the subjects, and the present study was approved by the Ethics Committee of of Peking University School and Hospital of Stomatology. All of the following experiments were performed in triplicate and repeated three times.

2.3.2. Cell adhesion and proliferation

A quantitative colorimetric cell counting kit-8 assay (CCK-8; Dojindo, Kyushu, Japan) was performed to characterize the adhesion and proliferation of HGFs. Cells were seeded onto the disks with or without PDA modification at a density of 10^5 cells per disk. After incubation for 3 h, 1 day, 3 days, 5 days, or 7 days, the samples were washed with PBS three times. CCK-8 diluted with cell culture medium (1:9 ratio by volume) was added to each well, followed by a 2-h incubation at 37 °C, and the supernatant was then transferred from the 24-well to 96-well cell culture plates. The optical density of the supernatant was measured using a spectrophotometer (ELX808; BioTek, Winooski, USA) at a wavelength of 450 nm.

2.3.3. Cell spreading and morphology

2.3.3.1. Confocal laser scanning microscopy (CLSM) of fibroblasts. HGFs were seeded at an initial density of 1.5×10^4 cells per disk onto the substrates and incubated for 3 h and 24 h. Subsequently, the unattached cells were rinsed off with sterile PBS. The attached cells were then fixed in 4% paraformaldehyde for 20 min and permeabilized in 0.1% Triton X-100 for 10 min at room temperature. Non-specific binding was then blocked with 1% bovine serum albumin (BSA; Sigma, St. Louis, USA) for 45 min. Thereafter, the samples were stained with fluorescein isothiocyanate–phalloidin (actin filament green color; Sigma). After extensive rinsing in PBS (3×, 5 min each), a drop of Fluoroshield containing 4',6-diamidino-2-phenylindole (nuclei blue color; Sigma) was added, and coverslips were mounted on the disks. Finally, the samples were observed by CLSM (LSM710; Zeiss, Germany). The cell area and perimeter were evaluated using an image analyzer (Image J, version 2, NIH).

2.3.3.2. SEM of fibroblasts. The substrates were seeded with HGFs at a density of 1.5×10^4 cells per disk. After 3 and 24 h, the non-adherent cells were rinsed off using PBS. The attached cells were then fixed with 2.5% glutaraldehyde for 2 h at 4 °C and rinsed three times in 0.1 M PBS for 15 min. Samples were then dehydrated with graded ethanol solutions (30, 50, 70, 80, 90, 95, and 100%) each for 5 min, followed by drying with hexamethyldisilazane (HMDS; JT Baker, Center Valley, USA) for 15 min. Finally, the samples were gold-sputtered and imaged by SEM.

2.3.4. Protein determination

The functional activity of the HGFs on the substrates was evaluated by measuring the matrix secreted by the cells after 3 and 7 days of incubation, with an initial seeding density of 10^5 cells per well. The amount of human collagen type I (Col-I) released from the cells into the culture medium was measured using an enzyme-linked immunosorbent assay kit (ELISA; R&D Systems, USA) in accordance with the manufacturer's instructions. Briefly, the supernatant was collected at the predetermined time points, centrifuged at 3000 rpm at 4 °C to remove particles, and was added at a 1:5 dilution in sample diluent into the 96-well plate together with 100 μl of conjugate reagent per well, followed by a 1-h incubation at 37 °C. The wells were then washed with washing buffer five times. Thereafter, 50 μl of substrate A and B were successively added into each well and maintained in the dark at 37 °C for 15 min. The optical density at 560 nm was measured using a spectrophotometer. The concentrations of the samples were determined using a standard curve established using standards of known concentrations.

2.3.5. Gene expression

Real-time polymerase chain reaction (PCR) was performed to determine the expression of adhesion- and differentiation-related genes in the HGFs. After finishing culturing at the pre-set time point (1 day, 3 days, or 7 days), HGFs were allowed to reach 80% confluence. Total RNA was extracted from the cultured cells using TRIzol reagent (Invitrogen) following the manufacturer's protocol and quantified using a biophotometer (Eppendorf, Germany). First-strand cDNA was synthesized from 2 μg of total RNA for each sample using the RevertAid First Strand cDNA Synthesis Kit (Thermo Scientific, Waltham, USA). To determine the mRNA levels of various integrins (α_2, α_5, β_1, and β_3), fibronectin (FN), Col-I, and glyceraldehyde phosphate dehydrogenase (GADPH), real-time PCR reactions were performed on a 7500 Real-time PCR System (Applied Biosystems, USA) using the Power SYBR Green PCR Master Mix (Applied Biosystems) with the specific primers previously described [9,23]. GADPH was used as the housekeeping gene. The relative expression levels are shown as fold differences relative to the results of the untreated surface and were calculated using the comparative DDCT method.

2.4. Bacterial response

2.4.1. Saliva coating of zirconia disks

Saliva was collected as described previously [39]. In brief, unstimulated whole saliva was collected on ice from ten healthy donors and pooled. The saliva was immediately cleared by centrifugation at 3000 × g for 20 min at 4 °C. The clarified saliva supernatant was diluted with distilled water (1:3 ratio by volume). The 25% saliva was then passed through a 0.20 μm filter and stored at −80 °C until use. Immediately before use, the sterile saliva was thawed at 37 °C and centrifuged again at 1430 × g for 5 min. Zirconia disks were then immersed in the clear supernatant for 2 h at 37 °C followed by a short rinse with distilled water.

2.4.2. Bacterial culture

Streptococcus gordonii (clinical isolate, Central Laboratory of Peking University School and Hospital of Stomatology) and *Streptococcus mutans* (UA159, provided by the institute of microbiology at the chinese academy of sciences) were maintained on a brain-heart infusion (BHI) agar plate (Oxoid, Basing-stoke, UK). A monoclonal colony was transferred to 10 ml of BHI broth culture medium and

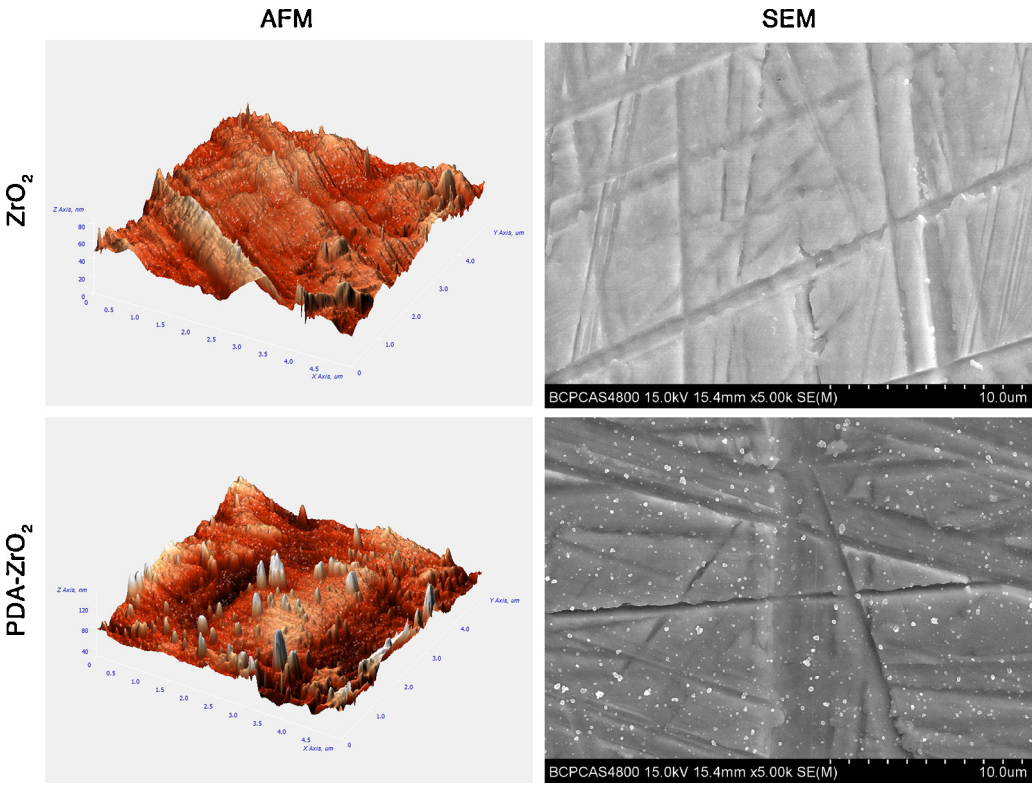

Fig. 1. Surface topography of zirconia substrates: AFM and SEM images of the pristine and PDA-coated zirconia.

cultivated aerobically for 12 h at 37 °C in an atmosphere containing 5% CO_2. Bacterial cells were collected during exponential phase growth by centrifugation at 3000 × g for 15 min. The bacterial pellet was washed twice with 0.15 M PBS buffer (pH 7.2). Bacteria were resuspended in the same buffer and the final concentration of each strain was adjusted to 5×10^7 CFU/ml. Immediately before seeding, the suspensions were sonicated for 30 s at 100 W to get single cells or pairs. A 2-ml aliquot of each cell suspension was added to a 24-well plate containing the sterilized samples and incubated for 2 h at 37 °C. After removing the culture medium, the cells were washed gently with sterile PBS solution three times to remove non-attached cells. Next, the adherent bacteria were subjected to various measurements, each of which was repeated three times.

2.4.3. Bacterial adhesion

Zirconia disks colonized with bacteria were prepared for SEM observation. Disks were fixed with 2.5% glutaraldehyde for 1 h at room temperature, washed 3 times with PBS buffer and then dehydrated through a graded series of ethanol (30, 50, 70, 80, 90, 95, and 100%) each for 5 min. Discs were subsequently dried, sputter-coated with gold, and imaged by SEM.

In the second trial, the morphologies and numbers of bacteria on zirconia disks were assessed using CLSM. The BacLight live/dead bacterial viability kit (L-7012, Invitrogen, USA) was used to examine both the live (green-fluorescent) and dead cells (red-fluorescent). The staining components A (SYTO 9) and B (propidium iodide) were mixed and diluted with PBS at a volume ratio of 1.5:1000, according to the manufacturer's protocol. Two hundred milliliters of staining solution were added to each sample, followed by incubation for 15 min at room temperature in the dark. The stained bacteria were observed using CLSM at 100-fold magnification and five digital images were taken from different areas on each surface for bacterial counting. Percentage of area covered by bacteria was calculated using Image J software.

2.5. Statistical analysis

All data were obtained from three repeated experiments performed in triplicate. Student's *t*-test was used for comparisons between the surfaces of the untreated and PDA-coated groups, and the level of significance (α) was set at 0.05. The confidence level was set as 95%. Data analyses were performed using the SPSS software (ver. 13.0; SPSS Inc., Chicago, IL, USA).

3. Results

3.1. Material surface analysis

The surface morphologies of zirconia and PDA-zirconia were investigated using SEM and AFM. As shown in Fig. 1, partial aggregates of polymerized dopamine were observed on PDA-zirconia, confirming the PDA coating. In addition, the surface roughness was determined by AFM (Supplementary table 1). After coating with PDA, the Ra value was slightly increased from 0.065 ± 0.022 to 0.071 ± 0.026; however, the difference between the modified and unmodified zirconia was not significant. Surface wettability was determined using contact angle measurements (Supplementary table 1). The water contact angle of pristine zirconia ($78 \pm 4°$) decreased to $64 \pm 1°$ after PDA coating.

XPS analysis of native zirconia substrates showed strong peaks of Zr 3d, O 1s, C 1s, as well as smaller peaks of Ca 2p3, N 1s, Y 3d (Fig. 2a). The significant increase in the relative intensity of N 1s suggested the successful coating of PDA onto the zirconia surface. Moreover, the suppression of the Zr 3d peak indicated that the most of the surface of zirconia had been covered by the PDA film.

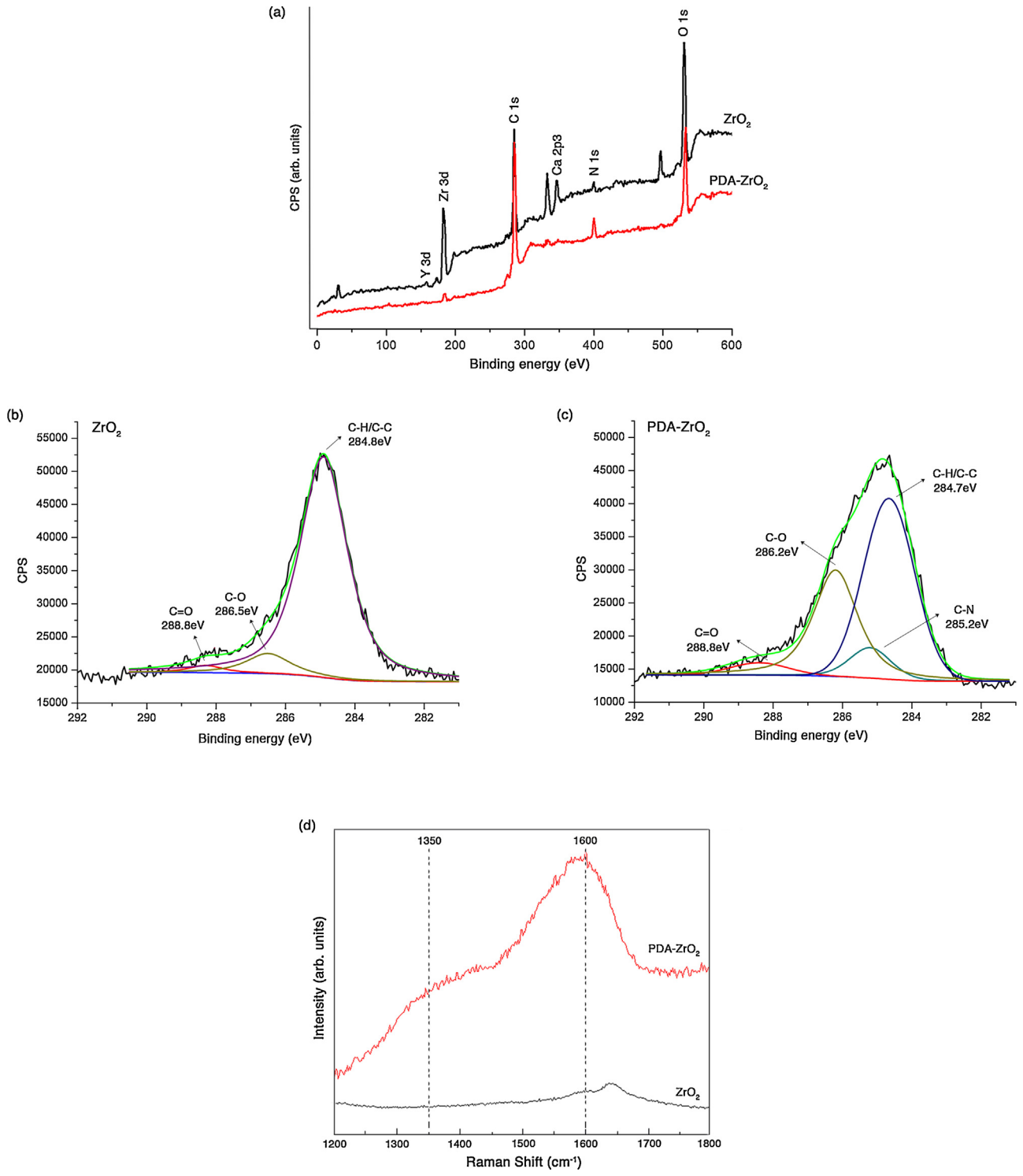

Fig. 2. XPS and Raman spectra: (a) XPS wide-scan spectra of zirconia and PDA-zirconia; (b)(c) typical high-resolution XPS C 1s spectra for pristine and PDA-coated zirconia; (d) Raman spectra of pristine and PDA-coated zirconia.

These results were confirmed by the data of elemental percentage changes summarized in Supplementary table 2. The concentrations of carbon and nitrogen increased dramatically from 59.43% and 3.4% on pristine zirconia to 72.33% and 6.68% after PDA coating, while the percentage of zirconium decreased from 7.23% to 0.77%. Figures 2b and c presented the high-resolution XPS C 1s spectra for the unmodified and PDA-coated zirconia. C 1s of native zirconia was deconvoluted into three components with binding energy at 284.8 eV (C—C/C—H), 286.5 eV (C—O), and 288.8 eV (C=O). After PDA coating, a peak assigned to the C—N bond appeared at about 285.2 eV. Additionally, the peaks of C—O (in the catechol) and C=O (in the dopaminequinone) increased and the intensity of C—C/C—H (in the benzene ring) decreased dramatically after PDA modification. The changes of percentages of functional groups were presented as Supplementary table 3. All these results suggested the presence of PDA on zirconia.

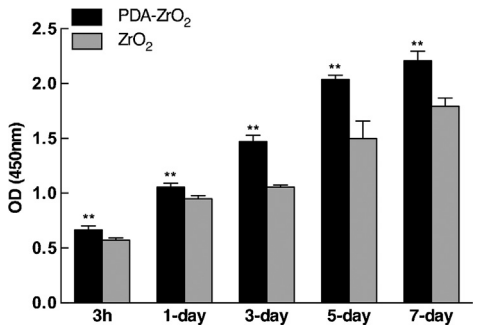

Fig. 3. The cell attachment and proliferation of HGFs cultured for 3 h, 1, 3, 5, and 7 days measured by a CCK-8 assay, with the pristine and PDA-coated zirconia. Data are shown as mean ± SD ($n = 9$). * represents $p < 0.05$ and * * represents $p < 0.01$, compared with the pristine zirconia.

In Raman spectra (Fig. 2d), characteristic peaks appeared at 1350 (stretching of catechol) and 1600 cm^{-1} (deformation of catechol) after PDA coating, in addition to intrinsic substrate peaks. These data confirmed that the zirconia surfaces were successfully coated with PDA.

3.2. Cell adhesion and proliferation analysis

The optical density of attached HGFs at 3 h and 1, 3, 5, and 7 days of incubation was significantly higher in the PDA-zirconia group than in the pristine zirconia group ($p < 0.01$) (Fig. 3). The two groups showed the greatest difference after 3 days of culture.

3.3. Cell morphology analysis

At 3 h of incubation, HGFs were attached to the surfaces in all of the groups (Fig. 4A and B). HGFs grown on pristine zirconia showed a small spherical shape, a typical non-spreading morphology. However, on PDA-zirconia, cell membrane protrusions were observed, and cells spread over a larger area. Subsequently, cell pseudopodia formed further, resulting in rapid cell spreading and formation of bridge connections between adjacent cells on PDA-zirconia after 24 h of culture. The HGFs of the control group, by contrast, displayed spindle-like and narrow morphology with little protrusions and a decreased number of cells. The mean spreading area and perimeter of adhered cells were further quantified (Fig. 4C); both the projected area and perimeter of HGFs were enhanced in the PDA-zirconia group. SEM analysis also demonstrated that HGFs showed a high degree of adhesion and spreading on PDA-modified disks (Fig. 4B). These results indicated that the PDA coating on zirconia substrates is conducive to cell attachment and spreading.

3.4. Protein synthesis analysis

The Col-I level in HGF culture medium at 3 and 7 days of incubation was measured (Fig. 5). HGFs cultured on PDA-zirconia displayed a significantly higher ($p < 0.05$) level of Col-I release than those on native zirconia after incubation for 7 days. The collagen level was slightly higher in the PDA-treated group after 3 days of culture, albeit not significantly so.

3.5. Gene expression analysis

The expression of biomarkers of HGF adhesion on zirconia is shown in Figure 6a. The HGFs in the PDA-zirconia group showed increased expression levels of the genes encoding integrin α_5, β_1, β_3 and FN, and a decreased level of that encoding integrin α_2, compared with the native zirconia group at 1 day of incubation. The expression of the cell-differentiation-related gene Col-I was higher in the PDA-modified group compared with the control group after culture for 3 and 7 days (Fig. 6b).

3.6. Microbiological analysis

S. gordonii and *S. mutans* colonization of zirconia substrates is shown in Fig. 7. For both SEM and CLSM, the modification of zirconia with PDA led to a marked decrease in the density of both *S. gordonii* and *S. mutans* adhesion (the sum of live and dead bacteria in CLSM), compared with that in the control group. The percentage of bacterial adhesion area to the tested surfaces is shown in Fig. 8. The PDA coated zirconia showed both lower percentages of *S. gordonii* (0.91 ± 0.16%) and *S. mutans* (1.85 ± 0.48%) than the pristine zirconia (1.73 ± 0.32% and 3.06 ± 0.47%) ($p < 0.01$), suggesting that the PDA coating resulted in significant reduction in bacterial adhesion.

4. Discussion

Due to its excellent aesthetic properties and biocompatibility, zirconia has been widely used as an abutment material for dental implants. However, to improve the soft-tissue integration around abutments, surface modifications are required. In the present study, we modified the zirconia surface with PDA, established a novel *in vitro* model using primary HGFs, *S. gordonii* and *S. mutans*, and evaluated their biological response to PDA-modified zirconia. The results indicated that PDA was successfully deposited on the surface of yttrium-stabilized zirconia and improved its bioactivity. The PDA coating has the following advantages: it is economic efficient, environmentally friendly, and simple to apply; there is no restriction on the shape and size of the substrates; and it facilitates further functionalization by grafting of biomolecules onto the PDA film.

To mimic the trans-gingival surface of commercially available zirconia abutments, we prepared zirconia disks with a smooth surface (Ra = 0.065). After dopamine coating, the surface roughness of the zirconia was not significantly changed, but the contact angle decreased significantly. These results are in agreement with those in previous reports [32]. In addition, in both XPS and Raman spectroscopy studies, the characteristic peaks corresponding to the elements or functional groups specific for dopamine were present. These results confirmed the successful functionalization of zirconia with PDA.

Effective HGF attachment to the implant materials plays an important role in the surrounding soft-tissue integration [6]. This study evaluated the effects on HGF adhesion, proliferation, morphology, protein synthesis, and expression of related genes of PDA coating of zirconia. Generally, cells undergo a cascade of events during adhesion onto a biomaterial surface: attachment, spreading, cytoskeleton development, and formation of cell-matrix adhesions. Upon exposure to the material surface, the initial step is cell attachment, which has a considerable impact on their subsequent reactions [40]. Several *in vitro* studies have demonstrated that PDA increased the attachment and spreading of various cell lines on a variety of substrates [33–35,37,41]. Our findings of enhanced HGF adhesion, spreading and proliferation on the PDA-coated surface are in line with these reports. The mechanism underlying the enhancement of cell adhesion by PDA coating is not well understood. According to previous studies, PDA reacts with substances containing amino and sulfhydryl groups via Schiff-base or Michael addition chemistry, thus adsorbing adhesive serum proteins such as FN. The adsorbed proteins maintain their native structure and serve as recognition sites for cell adhesion [33]. The surface wettability likely played no role in the PDA-mediated cell adhesion enhancement [34]. Wang et al. [41] evaluated the initial adhesive behavior of human umbilical vein endothelial cells on the PDA coating and

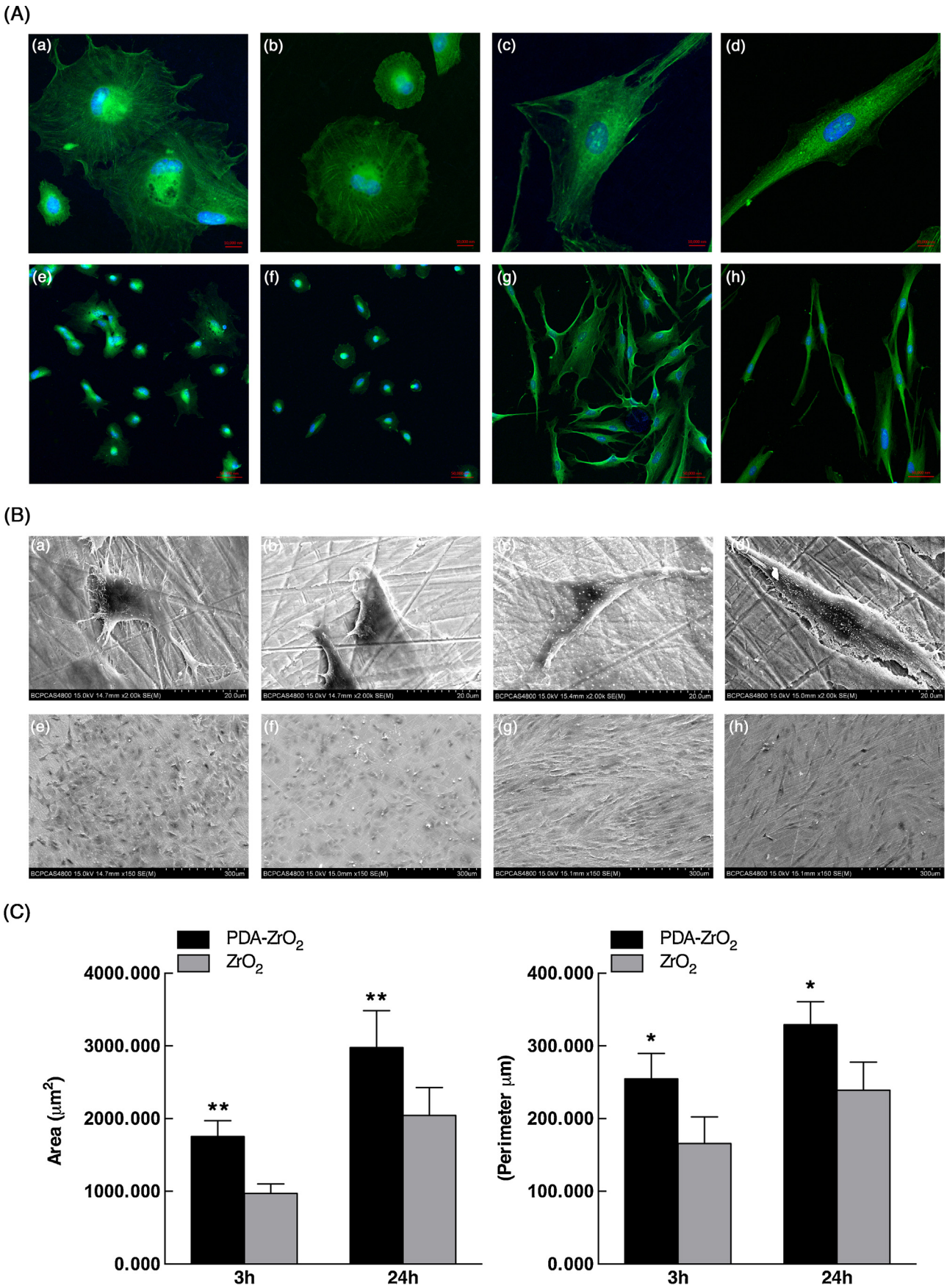

Fig. 4. Confocal laser scanning microscopy (A) and SEM (B) images of HGFs on pristine and PDA-coated zirconia at 3 h (a, b, e, f) and 24 h (c, d, g, h) of culture. High magnification: (a, c) PDA-ZrO_2, (b, d) ZrO_2, scale bar = 10 μm (A) and 20 μm (B). Low magnification: (e, g) PDA-ZrO_2, (f, h) ZrO_2, scale bar = 50 μm (A) and 300 μm (B). (C) The spreading areas and perimeters of HGFs on zirconia and PDA-zirconia surfaces. Data are shown as mean ± SD (n = 15). * represents $p < 0.05$ and * * represents $p < 0.01$, compared with the pristine zirconia.

found that FN and integrin α_5, β_1 were involved in the adhesion process. However, the gene expression data were qualitative, and whether the expression level of the corresponding gene in the PDA treatment group was higher than that in the control group was unclear. In this study, we explored the mechanism of adhesion of HGFs to PDA quantitatively using real-time PCR. The expression levels of integrin α_2, α_5, β_1, and β_3 were investigated because they have been identified in gingival tissue and play a predominant role in cell adhesion [23,40]. FN was also selected because, as an extracellular matrix protein, it plays a major role in cell attachment through interactions with integrins [42]. The results showed that the expression of the integrin α_5, β_1, β_3 and FN genes on PDA-zirconia was significantly upregulated compared with on native zirconia. By contrast, the expression of integrin α_2 was decreased on PDA-treated zirconia. These results suggested that the enhancement of HGF adhesion and spreading was attributable mainly to integrin α_5, β_1, β_3 and FN. Considering the relevant studies on integrin-mediated enhancement of cell biological activity, the combined upregulation of the integrin α_5, β_1, and FN genes indicated that HGFs on PDA-zirconia exhibited greater FN matrix assembly (fibronectin fibrillogenesis) and fibrillar adhesion than did cells in the zirconia group. Taking the upregulation of integrin β_3 into account, HGFs in the PDA-coated group may perform, or more actively perform three-dimensional matrix adhesion compared with cells in the control group. Three-dimensional-matrix interactions likely enhance the biological activity of cells [43]. Integrin α_2 is a collagen receptor needed for matrix remodeling and increased levels are associated with a fibrotic phenotype. That may be the reason of downregulation of Integrin α_2 after PDA coating. However, the expression of other factors, such as paxillin and focal adhesion kinase, must be assessed to draw firm conclusions on this matter.

The CCK-8 proliferation assay suggested that HGFs adhered and proliferated significantly more rapidly on PDA-coated than on native zirconia. In addition, PDA coating promoted cell spreading and resulted in an appropriate morphology. These data suggested that PDA coating enhanced the biologic responses of HGFs – such as attachment, proliferation and spreading – which are consistent with the aforementioned gene expression data.

Following implant surgery, HGFs are involved in the formation of connective tissue during wound healing by production of extracellular matrix factors, such as collagen type I [44]. Therefore, we analyzed the expression of Col-I, at both the gene and protein levels, to investigate the functional development of HFGs on PDA-zirconia. At both gene and protein levels, HGFs grown on PDA-zirconia exhibited slightly or significantly higher levels of Col-I at 3 and 7 days of incubation. These results indicate that PDA coating of zirconia may enhance HGF differentiation.

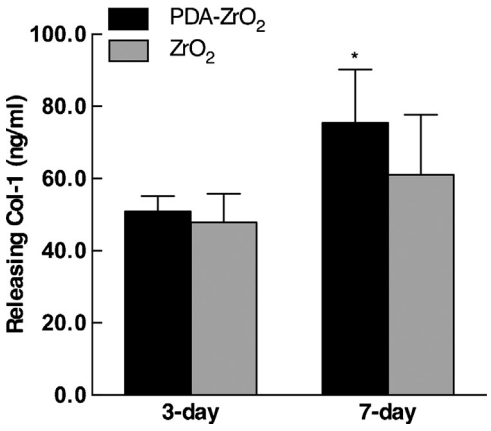

Fig. 5. The amount of Col-I releasing into the culture medium of zirconia and PDA-zirconia groups at 3 and 7 days of culture. Data are shown as mean ± SD ($n = 9$). * represents $p < 0.05$, compared with the pristine zirconia.

Taken together, the results show that high expression of integrins, particularly $\alpha_5\beta_1$, promoted the early formation of a FN matrix, which provided binding sites for regulatory factors and structural support for cell adhesion, proliferation, spreading, as well as differentiation.

Early colonization of bacteria is the initial step and plays a crucial role in the formation of plaque biofilm, leading to the pathological process of infection [10]. Therefore, decreasing the initial bacterial adherence onto implant surfaces during the early post-installment period plays a key role in the short- and long-term success of implantation. Our results indicated that the PDA modification significantly reduced *S. gordonii* and *S. mutans* adhesion onto the zirconia surface.

Surface roughness, surface energy, surface charge, and chemical composition appear to be correlated with bacterium-surface adhesion [12]. Regarding the influence of surface roughness, higher Ra values have been associated with increased plaque accumulation. However, an Ra value of 0.2 mm was suggested as a threshold, below which no further reduction in bacterial adhesion occurred [45]. In the present study, although the surface roughness of PDA-coated zirconia was slightly increased, the Ra value was less than 0.2 μm; therefore, the impact on bacterial adhesion was likely negligible. Many previous studies have shown that surfaces with

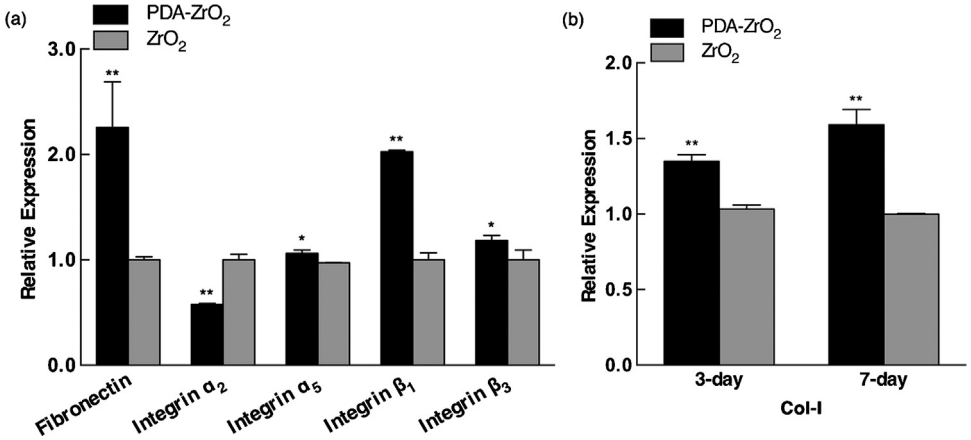

Fig. 6. Analysis on the expression of genes involved in HGF adhesion after 1 day of culture (a) and differentiation after 3 and 7 days of culture (b) in real-time PCR. Data represent fold changes of target genes normalized to GAPDH expressed relative to HGFs grown on pristine zirconia (100%). The values are expressed as mean ± SEM. * represents $p < 0.05$ and * * represents $p < 0.01$, compared with the pristine zirconia.

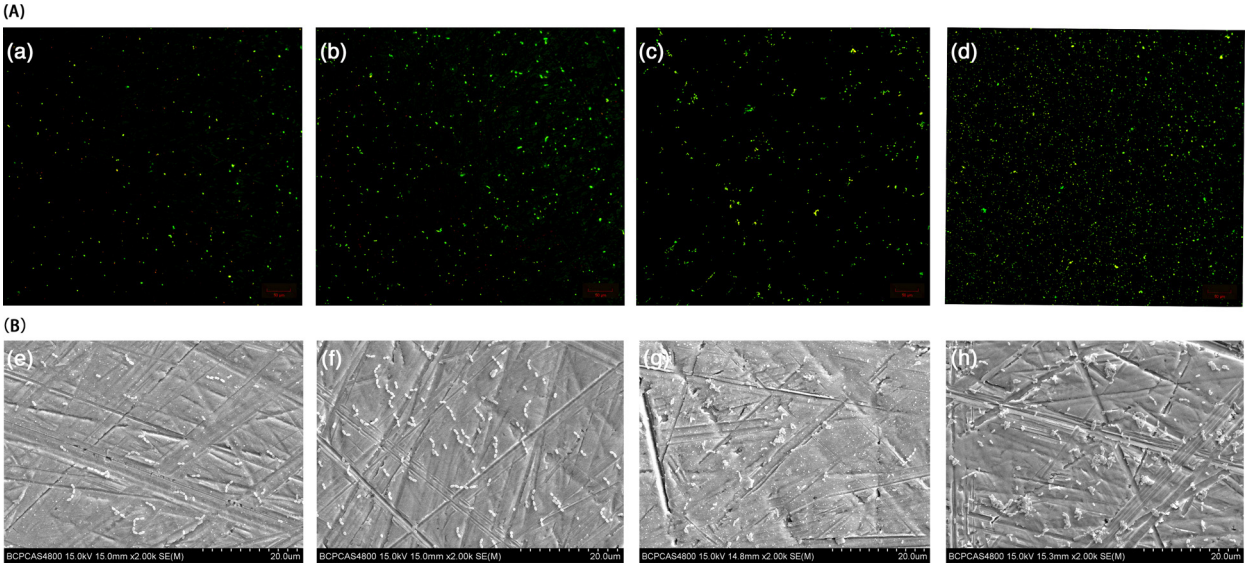

Fig. 7. Confocal laser scanning microscopy (A) and SEM (B) images of *S. gordonii* (a, b, e, f) and *S. mutans* (c, d, g, h) on pristine and PDA-coated zirconia at 2 h of culture. *S. gordonii*: (a, e) PDA-ZrO_2, (b, f) ZrO_2, scale bar = 50 μm (A) and 20 μm (B). *S. mutans*: (c, g) PDA-ZrO_2, (d, h) ZrO_2, scale bar = 50 μm (A) and 20 μm (B).

a higher surface energy are more prone to bacterial adherence [46,47]. However, several investigations on *streptococcal* strains have reported conflicting results [48,49]. The authors reported that charge interactions play a major role in early bacterial adhesion when the surface free energy increases. In addition, these studies suggested that the contributions of the various factors to oral bacterial adhesion onto dental materials may vary according to the bacterial species in question.

Dopamine compound exhibits antibacterial activity against certain bacteria, such as *E. coli* and *Staphylococcus aureus* [50]. Recently, Iqbal et al. [36] found that PDA has an antibacterial effect against *E. coli*. The effect was related to the cells being coated with PDA layer, which restricts the space for growth and multiplication or exerts local toxic effects on the outer membrane that caused changes in fluidity. Another explanation is that organic compounds such as quaternary ammonium salts might have an antimicrobial effect by a mechanism of increasing membrane permeation and the loss of membrane integrity. In these investigations, the bacteria were coincubated with dopamine solution. However, the intrinsic antimicrobial activity of the PDA film, which was used for modification of biomaterial surfaces, was rarely investigated. In most studies, PDA was used as an interface for binding other antibacterial factors, and the PDA-coated surface was used as a control. Among these few studies, He et al. [51] assessed the effects of RGD-, collagen- and dopamine-modified glass on *E. coli* and *S. aureus* adhesion. The research found that PDA-modified glass enhanced bacterial adhesion. Sileika et al. [52] investigated the antibacterial performance of PDA-modified polymer/metal surfaces. The results suggested that PDA coating led to a modest increase in the attachment of *E. coli* as well as *Pseudomonas aeruginosa* and a slight decrease in that of *Staphylococcus epidermidis*. In the first study, the surfaces become more hydrophobic after PDA modification, the opposite of our findings. In the second study, among the three bacterial strains investigated, only *S. epidermidis* was Gram positive and showed a similar pattern to *S. mutans* in terms of maintaining its homeostasis in response to environmental pH changes, which may explain their similar response to the PDA coating. In the present study, the intrinsic effect of PDA film on adhesion of oral bacteria was investigated for the first time. The adhesion of *S. gordonii* and *S. mutans* to zirconia surface decreased significantly after PDA coating. This might because the negatively charged (pH > 4) and

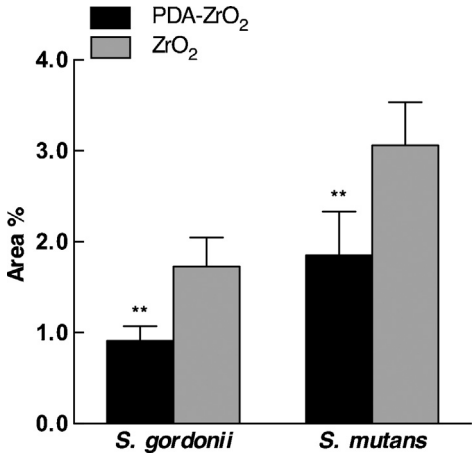

Fig. 8. Percentage of area covered by *S. gordonii* and *S. mutans* on zirconia and PDA-zirconia surfaces. Data are shown as mean ± SD ($n = 15$). * * represents $p < 0.01$, compared with the pristine zirconia.

relatively hydrophilic PDA coating reduced the adhesion of the negatively charged salivary protein and subsequent bacteria adhesion.

As a consequence, the results suggest acceptance of the research hypothesis, indicating that PDA is able to modify the surface of zirconia, improve HGFs' response and reduce bacterial adhesion. The integrin $\alpha_5, \beta_1, \beta_3$ and FN play an important role in the cell response improvement. However, mono-culture *in vitro* study is sometimes at odds with clinical reality. To avoid this, and better mimic what is called "the race for the surface" between tissue cells and bacteria, co-culture methods have been developed [53–55]. Therefore, further studies are required to clarify whether the PDA coating still works under co-culture condition and *in vivo* environment. Additionally, the safety and immune effect of PDA coating on human body need to be evaluated.

5. Conclusion

In this study, we present a simple, environmentally friendly, and effective surface modification technique for zirconia dental implant materials. Additionally, this study provides an approach for further functionalization of zirconia substrates via immobiliz-

ing other biomolecules. Within the limitations of this *in vitro* study, the results suggest that PDA coating of zirconia substrates enhances HGF responses and decreases bacterial activity. The PDA-modified zirconia thus shows promise for enhancing peri-implant soft-tissue integration in clinical application. However, the outcome of simultaneous bacterial colonization and tissue integration results remain to be seen, and further investigation in animal models are needed regarding whether this modification would also exhibits *in vivo* soft-tissue healing-promoting effects.

Acknowledgments

The study was supported by the National Natural Science Foundation of China (No. 81200807) and funding from Peking University School of Stomatology (YS020212). We have no conflict of interests for the study.

Appendix A. Supplementary data

Supplementary data associated with this article can be found, in the online version, at http://dx.doi.org/10.1016/j.colsurfb.2015.06.047.

References

[1] T. Berglundh, J. Lindhe, I. Ericsson, C.P. Marinello, B. Liljenberg, P. Thomsen, Clin. Oral Implants Res. 2 (1991) 81.
[2] R. Glauser, P. Schupbach, J. Gottlow, C.H. Hammerle, Clin. Implant Dent. Relat. Res. 7 (Suppl 1) (2005) S44.
[3] E. Rompen, O. Domken, M. Degidi, A.E. Pontes, A. Piattelli, Clin. Oral Implants Res. 17 (Suppl 2) (2006) 55.
[4] S.W. Lee, S.Y. Kim, I.C. Rhyu, W.Y. Chung, R. Leesungbok, K.W. Lee, Clin. Oral Implants Res. 20 (2009) 56.
[5] P.M. Bartold, L.J. Walsh, A.S. Narayanan, Periodontology 2000 (24) (2000) 28.
[6] I.S. Moon, T. Berglundh, I. Abrahamsson, E. Linder, J. Lindhe, J. Clin. Periodontol. 26 (1999) 658.
[7] B. Grossner-Schreiber, M. Herzog, J. Hedderich, A. Duck, M. Hannig, M. Griepentrog, Clin. Oral Implants Res. 17 (2006) 736.
[8] S. Miura, J. Takebe, J. Prosthodont. Res. 56 (2012) 178.
[9] M. Gomez-Florit, J.M. Ramis, R. Xing, S. Taxt-Lamolle, H.J. Haugen, S.P. Lyngstadaas, M. Monjo, J. Periodontal Res. 49 (2014) 425.
[10] K. Subramani, R.E. Jung, A. Molenberg, C.H. Hammerle, Int. J. Oral Maxillofac. Implants 24 (2009) 616.
[11] M.M. Furst, G.E. Salvi, N.P. Lang, G.R. Persson, Clin. Oral Implants Res. 18 (2007) 501.
[12] W. Teughels, N. Van Assche, I. Sliepen, M. Quirynen, Clin. Oral Implants Res. 17 (Suppl 2) (2006) 68.
[13] M. Yoshinari, Y. Oda, T. Kato, K. Okuda, Biomaterials 22 (2001) 2043.
[14] N. Ren, R. Li, L. Chen, G. Wang, D. Liu, Y. Wang, L. Zheng, W. Tang, X. Yu, H. Jiang, H. Liu, N. Wu, J. Mater. Chem. 22 (19) (2012) 151.
[15] B. Grossner-Schreiber, M. Griepentrog, I. Haustein, W.D. Muller, K.P. Lange, H. Briedigkeit, U.B. Gobel, Clin. Oral Implants Res. 12 (2001) 543.
[16] N. Villard, C. Seneviratne, J.K. Tsoi, M. Heinonen, J. Matinlinna, Clin. Oral Implants Res. (2014).
[17] L. Zhao, Y. Hu, D. Xu, K. Cai, Colloids Surf. B. Biointerfaces 119 (2014) 115.
[18] F. Zhang, Z. Zhang, X. Zhu, E.T. Kang, K.G. Neoh, Biomaterials 29 (2008) 4751.
[19] M. Kazemzadeh-Narbat, B.F. Lai, C. Ding, J.N. Kizhakkedathu, R.E. Hancock, R. Wang, Biomaterials 34 (2013) 5969.
[20] N.J. Hickok, I.M. Shapiro, Adv. Drug Deliv. Rev. 64 (2012) 1165.
[21] Z. Ozkurt, E. Kazazoglu, J. Oral Implantol. 37 (2011) 367.
[22] L. Rimondini, L. Cerroni, A. Carrassi, P. Torricelli, Int. J. Oral Maxillofac. Implants 17 (2002) 793.
[23] S. Yamano, A.K. Ma, R.M. Shanti, S.W. Kim, K. Wada, C. Sukotjo, Int. J. Oral Maxillofac. Implants 26 (2011) 1247.
[24] M. Bachle, F. Butz, U. Hubner, E. Bakalinis, R.J. Kohal, Clin. Oral Implants Res. 18 (2007) 53.
[25] Y. Yang, J. Zhou, X. Liu, M. Zheng, J. Yang, J. Tan, J. Biomed. Mater. Res. B Appl. Biomater. 103 (2014) 116.
[26] L. Hao, J. Lawrence, K.S. Chian, J. Mater. Sci. Mater. Med. 16 (2005) 719.
[27] S. Stubinger, F. Homann, C. Etter, M. Miskiewicz, M. Wieland, R. Sader, Lasers Surg. Med. 40 (2008) 223.
[28] Z. Zhang, K. Wang, C. Bai, X. Li, X. Dang, C. Zhang, Colloids Surf. B. Biointerfaces 89 (2012) 40.
[29] J. Lee, J.H. Sieweke, N.A. Rodriguez, P. Schupbach, H. Lindstrom, C. Susin, U.M. Wikesjo, J. Clin. Periodontol. 36 (2009) 610.
[30] H.W. Kim, Y.M. Kong, C.J. Bae, Y.J. Noh, H.E. Kim, Biomaterials 25 (2004) 2919.
[31] Y. Liu, K. Ai, L. Lu, Chem. Rev. 114 (2014) 5057.
[32] H. Lee, S.M. Dellatore, W.M. Miller, P.B. Messersmith, Science 318 (2007) 426.
[33] S.H. Ku, J. Ryu, S.K. Hong, H. Lee, C.B. Park, Biomaterials 31 (2010) 2535.
[34] Y.M. Shin, Y.B. Lee, H. Shin, Colloids Surf. B. Biointerfaces 87 (2011) 79.
[35] W.B. Tsai, W.T. Chen, H.W. Chien, W.H. Kuo, M.J. Wang, Acta Biomater. 7 (2011) 4187.
[36] Z. Iqbal, E.P.C. Lai, T.J. Avis, J. Mater. Chem. 22 (2012) 21608.
[37] Y.T. Liu, T.M. Lee, T.S. Lui, Colloids Surf. B. Biointerfaces 106 (2013) 37.
[38] Z.-Y. Xi, Y.-Y. Xu, L.-P. Zhu, Y. Wang, B.-K. Zhu, J. Membr. Sci. 327 (2009) 244.
[39] M. Kuboniwa, A. Amano, E. Hashino, Y. Yamamoto, H. Inaba, N. Hamada, K. Nakayama, G.D. Tribble, R.J. Lamont, S. Shizukuishi, BMC Microbiol. 9 (2009) 105.
[40] U. Hersel, C. Dahmen, H. Kessler, Biomaterials 24 (2003) 4385.
[41] J.L. Wang, K.F. Ren, H. Chang, F. Jia, B.C. Li, Y. Ji, J. Ji, Macromol. Biosci. 13 (2013) 483.
[42] S.K. Sastry, K. Burridge, Exp. Cell Res. 261 (2000) 25.
[43] E. Cukierman, R. Pankov, D.R. Stevens, K.M. Yamada, Science 294 (2001) 1708.
[44] A.A. Palaiologou, R.A. Yukna, R. Moses, T.E. Lallier, J. Periodontol. 72 (2001) 798.
[45] C.M. Bollen, P. Lambrechts, M. Quirynen, Dent. Mater. 13 (1997) 258.
[46] J. van Dijk, F. Herkstroter, H. Busscher, A. Weerkamp, H. Jansen, J. Arends, J. Clin. Periodontol. 14 (1987) 300.
[47] M. Quirynen, C.M. Bollen, J. Clin. Periodontol. 22 (1995) 1.
[48] S. Hahnel, M. Rosentritt, G. Handel, R. Burgers, Dent. Mater. 25 (2009) 969.
[49] A.H. Weerkamp, H.M. Uyen, H.J. Busscher, J. Dent. Res. 67 (1988) 1483.
[50] M. Friedman, R. Buick, C.T. Elliott, J. Food Prot. 67 (2004) 1774.
[51] T. He, Z.L. Shi, N. Fang, K.G. Neoh, E.T. Kang, V. Chan, Biomaterials 30 (2009) 317.
[52] T.S. Sileika, H.D. Kim, P. Maniak, P.B. Messersmith, ACS Appl Mater. Interfaces 3 (2011) 4602.
[53] H.J. Busscher, H.C. van der Mei, G. Subbiahdoss, P.C. Jutte, J.J. van den Dungen, S.A. Zaat, M.J. Schultz, D.W. Grainger, Sci. Transl. Med. (2012) 153rv10.
[54] G. Subbiahdoss, R. Kuijer, D.W. Grijpma, H.C. van der Mei, H.J. Busscher, Acta Biomater. 5 (2009) 1399.
[55] B. Zhao, H.C. van der Mei, G. Subbiahdoss, J. de Vries, M. Rustema-Abbing, R. Kuijer, H.J. Busscher, Y. Ren, Dent. Mater. 30 (2014) 716.